

Hadronic B decays and charm at Belle II

Sagar Hazra, on behalf of the Belle II collaboration
*Tata Institute of Fundamental Research,
Mumbai 400 005, India*



We report the measurements of various hadronic B decays and charm at the Belle II experiment using a 362 fb^{-1} sample of electron-positron collisions collected at the $\Upsilon(4S)$ resonance. All results are competitive with the previous determination, and some of them are already competitive with the world's best measurement.

1 Introduction

The study of hadronic B decays plays an important role in the flavor physics program to test the standard model (SM) and its extensions. Decays mediated by Cabibbo-suppressed $b \rightarrow u$ and $b \rightarrow d, s$ loop transitions constitute sensitive probes for non-SM contributions. We can exploit isospin symmetry in some hadronic decays to construct various sum rules. One such sum-rule combines the branching fractions and CP asymmetries of $B \rightarrow K\pi$ decays, providing a null test with precision better than 1% in the SM. Similarly, the CKM angle ϕ_2/α can be measured directly by an analysis of various $B \rightarrow \pi\pi$ decays related by isospin symmetry. Belle II has the unique capability of studying jointly, and within a consistent experimental environment, all relevant final states of isospin-related B decays to improve our knowledge of angle ϕ_2 as well as to put a stringent bound on the sum-rule test. The CKM angle ϕ_3/γ is an SM candle for CP violation and is very reliably predicted. A measurement of this angle has been performed in an analysis of the $B \rightarrow DK$ decays. Lastly, we report a novel charm flavor tagger that would be important for CP violation and mixing studies in the charm sector.

21 2 Determination of signal yield

22 A key challenge in signal reconstruction is the large contamination from $e^+e^- \rightarrow q\bar{q}$ ($q =$
 23 u, d, s, c) background coupled with a small signal branching fraction. We use a binary-decision-
 24 tree classifier that combines a number of mostly topological variables with some discrimination
 25 between the B -meson signal and $q\bar{q}$ background. To determine the signal yield, we rely on
 26 two kinematic variables: the energy difference $\Delta E = E_B^* - \sqrt{s}/2$ between the energy of the
 27 reconstructed B candidate and half the collision energy, and the beam-energy-constrained mass
 28 $M_{bc} = \sqrt{s/(4c^4) - (p_B^*/c)^2}$, which is the invariant mass of the B meson, with its energy being
 29 replaced by half the collision energy; all quantities are calculated in the $\Upsilon(4S)$ frame.

30 3 Isospin sum-rule

31 The isospin sum-rule relation for the $B \rightarrow K\pi$ system provides a stringent null test of the SM¹,

$$I_{K\pi} = \mathcal{A}_{K^+\pi^-} + \mathcal{A}_{K^0\pi^+} \frac{\mathcal{B}(K^0\pi^+) \tau_{B^0}}{\mathcal{B}(K^+\pi^-) \tau_{B^+}} - 2\mathcal{A}_{K^+\pi^0} \frac{\mathcal{B}(K^+\pi^0) \tau_{B^0}}{\mathcal{B}(K^+\pi^-) \tau_{B^+}} - 2\mathcal{A}_{K^0\pi^0} \frac{\mathcal{B}(K^0\pi^0)}{\mathcal{B}(K^+\pi^-)} = 0, \quad (1)$$

32 where \mathcal{B} , \mathcal{A} , and τ are the branching fraction, direct CP asymmetries, and lifetime of B decays,
 33 respectively. We measure the time-integrated asymmetry for the CP eigenstate $B^0 \rightarrow K^0\pi^0$ by
 34 inferring the B -meson flavor q from that of the other B meson produced on the $\Upsilon(4S)$ decay,
 35 using a category-based flavor tagger².

36 Figures 1 and 2 show the ΔE distribution of all the four $K\pi$ system. We obtain the following
 37 branching fractions,

$$\begin{aligned} \mathcal{B}(B^0 \rightarrow K^+\pi^-) &= [20.7 \pm 0.4(\text{stat}) \pm 0.6(\text{syst})] \times 10^{-6}, \\ \mathcal{B}(B^+ \rightarrow K^+\pi^0) &= [14.2 \pm 0.4(\text{stat}) \pm 0.9(\text{syst})] \times 10^{-6}, \\ \mathcal{B}(B^+ \rightarrow K^0\pi^+) &= [24.4 \pm 0.7(\text{stat}) \pm 0.9(\text{syst})] \times 10^{-6}, \\ \mathcal{B}(B^0 \rightarrow K^0\pi^0) &= [10.2 \pm 0.6(\text{stat}) \pm 0.6(\text{syst})] \times 10^{-6} \end{aligned}$$

38 and CP -violating rate asymmetries

$$\begin{aligned} \mathcal{A}_{CP}(B^0 \rightarrow K^+\pi^-) &= -0.07 \pm 0.02(\text{stat}) \pm 0.01(\text{syst}), \\ \mathcal{A}_{CP}(B^+ \rightarrow K^+\pi^0) &= 0.01 \pm 0.03(\text{stat}) \pm 0.01(\text{syst}), \\ \mathcal{A}_{CP}(B^+ \rightarrow K^0\pi^+) &= -0.01 \pm 0.08(\text{stat}) \pm 0.05(\text{syst}), \\ \mathcal{A}_{CP}(B^0 \rightarrow K^0\pi^0) &= -0.06 \pm 0.15(\text{stat}) \pm 0.05(\text{syst}). \end{aligned}$$

The dominant contribution to the systematic uncertainties comes from the π^0 and K_S^0 recon-

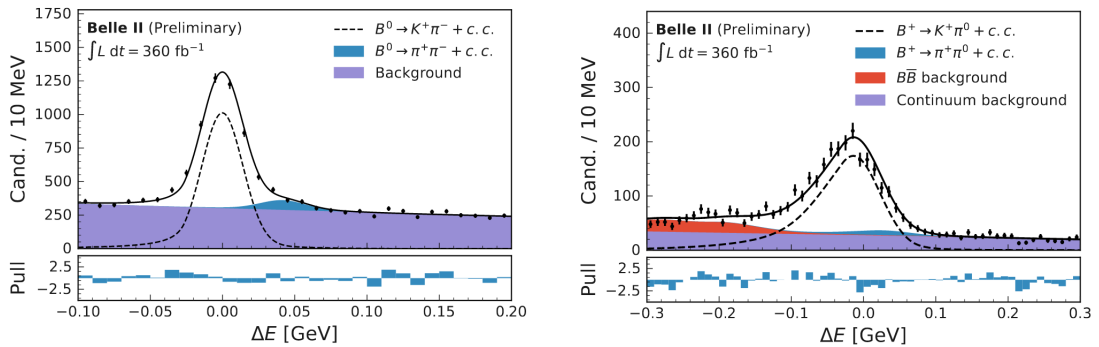


Figure 1 – Signal-enhanced ΔE distributions of $B^0 \rightarrow K^+\pi^-$ (left) and $B^+ \rightarrow K^+\pi^0$ (right).

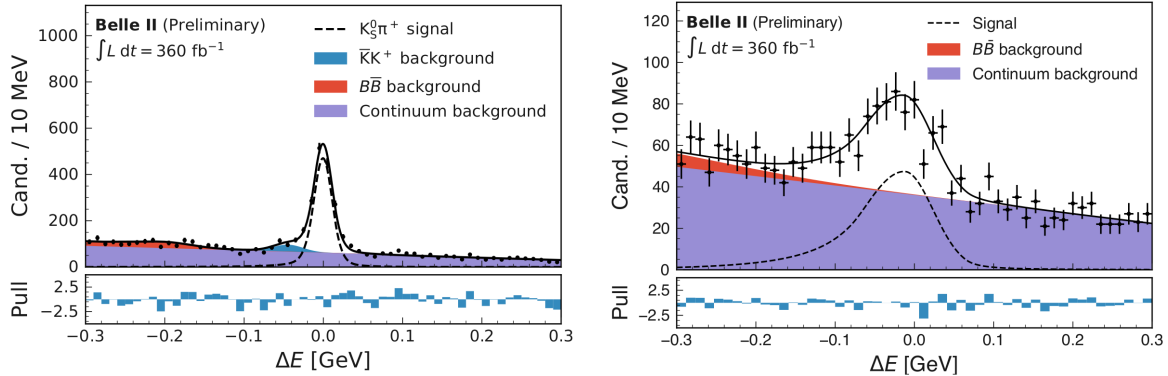


Figure 2 – Signal-enhanced ΔE distributions of $B^+ \rightarrow K^0\pi^+$ (left) and $B^0 \rightarrow K^0\pi^0$ (right).

39

39 construction efficiency for the decays having these final state particles. These are determined in the
 40 control sample of data and are expected to significantly decrease with a larger sample size.

42

42 We also measure CP asymmetry in $B^0 \rightarrow K_S^0\pi^0$ decays using a time-dependent method.
 43 Another motivation to perform this measurement is to prove the effective value of $\Delta\mathcal{S}_{CP} =$
 44 $\mathcal{S}_{CP} - \sin(2\phi_1)$ for the $b \rightarrow s$ loop transitions. The main challenge of this analysis is the absence
 45 of primary charged particles, which leads to poor decay time resolution. The analysis is validated
 46 with the $B^0 \rightarrow J/\psi K_S^0$ control sample, reconstructed with only the K_S^0 vertex. Figure 3 shows
 47 the ΔE and Δt distributions of the $B^0 \rightarrow K_S^0\pi^0$ time-dependent CP asymmetry measurement.
 48 We obtain

$$\mathcal{A}_{CP} = 0.04_{-0.14}^{+0.15}(\text{stat}) \pm 0.05(\text{syst})$$

49 and

$$\mathcal{S}_{CP} = 0.75_{-0.23}^{+0.20}(\text{stat}) \pm 0.04(\text{syst}).$$

50

50 Mixing-induced asymmetry parameter \mathcal{S}_{CP} is already competitive with the world's best mea-
 51 surement even with a smaller dataset.

52

52 We combine the time-dependent and time-integrated measurements to obtain the best sen-
 53 sitivity of $\mathcal{A}_{K_S^0\pi^0} = -0.01 \pm 0.12(\text{stat}) \pm 0.05(\text{syst})$. Putting all \mathcal{B} and \mathcal{A}_{CP} values of the $K\pi$
 54 system together, we obtain an overall Belle II isospin test:

$$I_{K\pi} = -0.03 \pm 0.13(\text{stat}) \pm 0.05(\text{syst}),$$

55

55 which is consistent with the SM prediction and comparable with world's best result (-0.13 ± 0.11)
 56 even with a smaller sample.

57

4 Towards the determination of ϕ_2

58

58 The combined analysis of branching fractions and CP violating asymmetries of the complete set
 59 of $B \rightarrow \pi\pi$ isospin partners enables a determination of ϕ_2 ³. We focus here on $B^+ \rightarrow \pi^+\pi^0$
 60 and $B^0 \rightarrow \pi^+\pi^-$ decays. Belle II has the unique capability to study all the $B \rightarrow \pi\pi$ decays to
 61 determine the CKM angle ϕ_2 . Figure 4 shows the ΔE distribution of two $\pi\pi$ channels.

62

We obtain the following branching fractions,

$$\begin{aligned} \mathcal{B}(B^0 \rightarrow \pi^+\pi^-) &= [5.83 \pm 0.22(\text{stat}) \pm 0.17(\text{syst})] \times 10^{-6}, \\ \mathcal{B}(B^+ \rightarrow \pi^+\pi^0) &= [5.02 \pm 0.28(\text{stat}) \pm 0.32(\text{syst})] \times 10^{-6}, \end{aligned}$$

63

63 and CP asymmetry of $\mathcal{A}_{CP}(B^+ \rightarrow \pi^+\pi^0) = -0.08 \pm 0.05(\text{stat}) \pm 0.01(\text{syst})$. The dominant
 64 contribution in the systematic uncertainties comes from π^0 reconstruction and tracking efficiency.

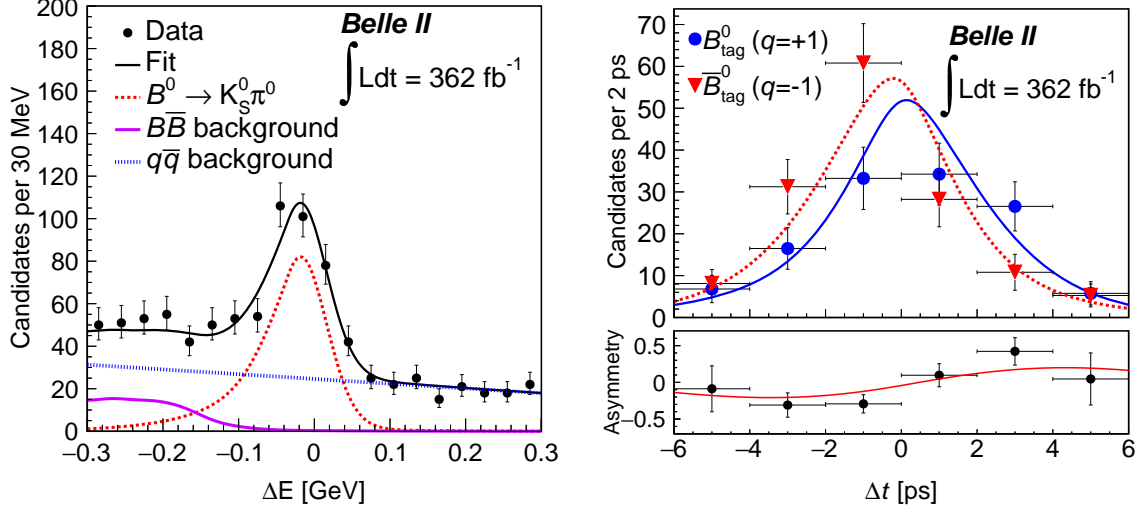


Figure 3 – Signal-enhanced ΔE distribution (left) and background subtracted B^0 and \bar{B}^0 -tag Δt distribution (right) for $B^0 \rightarrow K_s^0 \pi^0$ time-dependent CP asymmetry measurement.

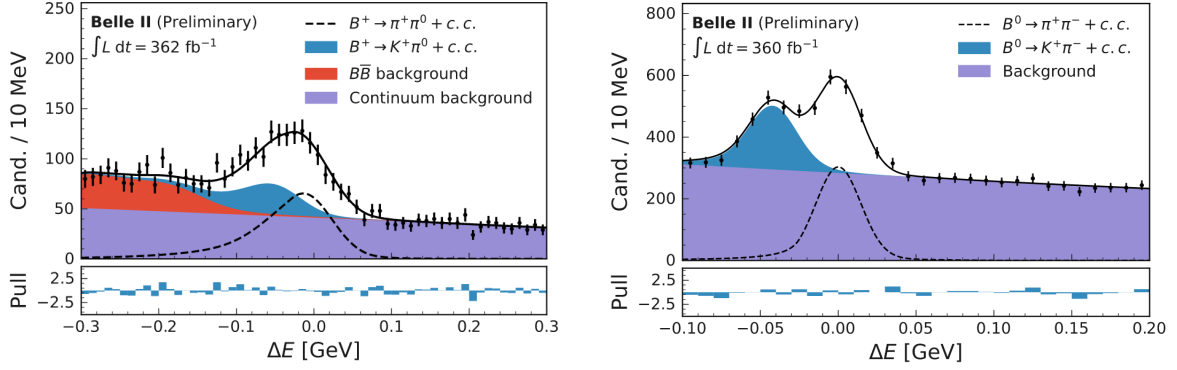


Figure 4 – Signal-enhanced ΔE distributions of $B^+ \rightarrow \pi^+ \pi^0$ (left) and $B^0 \rightarrow \pi^+ \pi^-$ (right).

65 5 Determination of ϕ_3/γ

66 The CKM unitary angle ϕ_3/γ is a SM benchmark as it is the only angle accessed at tree level.
 67 The angle ϕ_3 is governed by interference between the favoured $b \rightarrow c\bar{u}s$ and suppressed $b \rightarrow u\bar{c}s$
 68 transitions in the $B \rightarrow DK$ decays:

$$\frac{\mathcal{A}_{\text{sup}}(B^- \rightarrow \bar{D}^0 K^-)}{\mathcal{A}_{\text{fav}}(B^- \rightarrow \bar{D}^0 K^-)} = r_B e^{i(\delta_B - \gamma)}, \quad (2)$$

69 where δ_B is the strong phase difference and r_B is the magnitude of the suppression. The angle
 70 ϕ_3 measured using different methods based on a number of D final states. We present the
 71 determination of ϕ_3 using GLW^{4,5} and GLS⁶ method with Belle and Belle II dataset.

72 The GLW method uses the $D \rightarrow K^+ K^-$ (CP -even) and $D \rightarrow K_s^0 \pi^0$ (CP -odd) eigenstate to
 73 determine ϕ_3 from $\mathcal{R}_{CP\pm} = 1 + r_B^2 \pm 2r_B \cos \delta_B \cos \phi_3$ and $\mathcal{A}_{CP\pm} = \pm 2r_B \sin \delta_B \sin \phi_3 / \mathcal{R}_{CP\pm}$.
 74 This analysis used a combined Belle (711 fb^{-1}) and Belle II (189 fb^{-1}) data sample. While
 75 the results for CP -even eigenstate are not yet competitive with the world average, the CP -odd
 76 eigenstate results achieve world's best measurement as it is a unique channel for the Belle II.
 77 We find the following relative branching fractions,

$$\begin{aligned} \mathcal{R}_{CP+} &= (1.16 \pm 0.08(\text{stat}) \pm 0.04(\text{syst}))\%, \\ \mathcal{R}_{CP-} &= (1.15 \pm 0.07(\text{stat}) \pm 0.02(\text{syst}))\% \end{aligned}$$

78 and CP -violating rate asymmetries,

$$\begin{aligned}\mathcal{A}_{CP+} &= (+12.5 \pm 5.8(\text{stat}) \pm 1.4(\text{syst}))\%, \\ \mathcal{A}_{CP-} &= (-16.7 \pm 5.7(\text{stat}) \pm 0.6(\text{syst}))\%.\end{aligned}$$

79 The GLS method uses the Cabibbo-suppressed channels $B^\pm \rightarrow D(\rightarrow K_s^0 K^\pm \pi^\mp) h^\pm$ (same
80 sign) and $B^\mp \rightarrow D(\rightarrow K_s^0 K^\pm \pi^\mp) h^\mp$ (opposite sign) to determine 4 CP asymmetries and 3
81 branching ratios. This analysis used the combined Belle (711 fb^{-1}) and Belle II (362 fb^{-1}) data
82 sample. While the results are not competitive with world average, they still provide a constraint
83 on the measurement on ϕ_3 . This results will be used for the combination of ϕ_3 measurement
84 with Belle and Belle II data sample. We find the following ratio of branching fractions,

$$\begin{aligned}\mathcal{A}_{SS}^{DK} &= -0.089 \pm 0.091 \pm 0.011, \\ \mathcal{A}_{OS}^{DK} &= +0.109 \pm 0.133 \pm 0.013, \\ \mathcal{A}_{SS}^{D\pi} &= +0.018 \pm 0.026 \pm 0.009, \\ \mathcal{A}_{OS}^{D\pi} &= -0.028 \pm 0.031 \pm 0.009,\end{aligned}$$

85 and CP -violating rate asymmetries,

$$\begin{aligned}\mathcal{R}_{SS}^{DK/D\pi} &= 0.122 \pm 0.012 \pm 0.004, \\ \mathcal{R}_{OS}^{DK/D\pi} &= 0.093 \pm 0.013 \pm 0.003, \\ \mathcal{R}_{SS/OS}^{D\pi} &= 1.428 \pm 0.057 \pm 0.002.\end{aligned}$$

86 6 The charm flavor tagger

87 Identification of the D^0 and \bar{D}^0 flavor plays a crucial role in the CP -violation and mixing
88 measurement in the charm sector. Typically all the charm analysis uses the conventional D^* -
89 tagging method which has high purity but substantially reduces the data sample size. The
90 main motivation to develop new charm flavor is to increase the sample size. The new charm
91 flavor tagger uses boosted-decision-trees⁷ to recover additional flavor information from the extra
92 charged particles. Figure 5 shows a good agreement between the calibrated and true flavor
93 dilution. The novel charm flavor tagger has an effective tagging power,

$$\epsilon_{\text{tag}}^{\text{eff}} = (47.91 \pm 0.07(\text{stat}) \pm 0.51(\text{syst}))\%,$$

94 which is calculated in the $D^0 \rightarrow K^- \pi^+$ decays. Effective increase in the sample size is estimated
95 to evaluate the impact of charm flavor tagger in physics analysis. Figures 6 shows the effect of
96 charm flavor tagger on $D^* \rightarrow D^0[\rightarrow K^+ \pi^- \pi^0] \pi^+$ decays. We find for $D^0 \rightarrow K^- \pi^+$, doubling
97 the effective sample size compared to conventional D^* -tagged decays.

98 7 Conclusions

99 In summary, hadronic B decays and charm physics play an important role in sharpening flavor
100 picture. Belle II has unique access to channels that offer key tests of the SM. We have shown
101 five results new for this conference: CP violation in $B^0 \rightarrow K_s^0 \pi^0$ that probes isospin sum rule
102 with world leading precision, precise measurements of various two-body decays related to the
103 extraction of angle ϕ_2 , joining forces with Belle sample to offer most up-to-date information on
104 ϕ_3 from GLW and GLS analyses, novel neutral charm tagger that nearly doubles the tagged
105 sample size.

106 8 Acknowledgement

107 The author thanks to the Infosys Foundation for providing the leading edge travel grant.

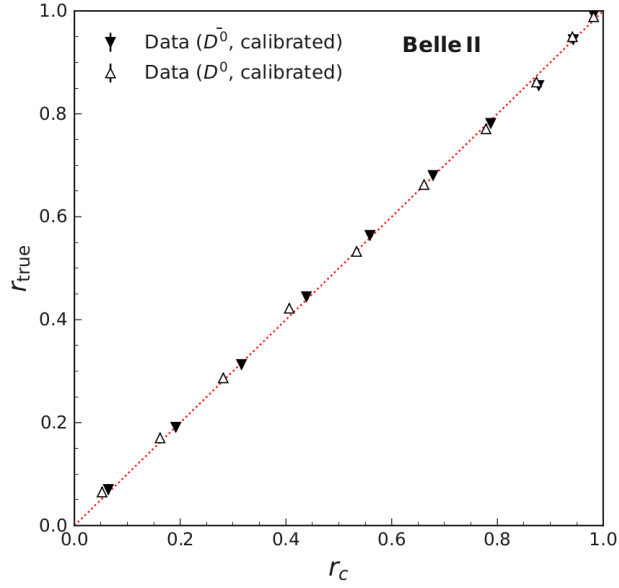


Figure 5 – True dilution as a function of calibrated dilution for $D^0 \rightarrow k^- \pi^+$ decays.

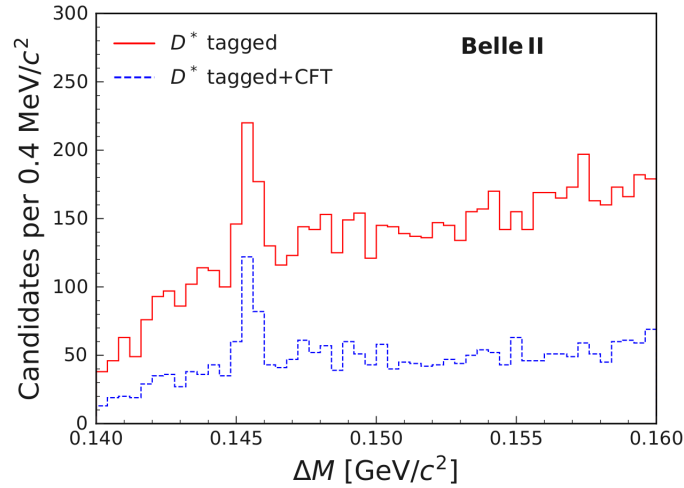


Figure 6 – Distribution of the difference between D^* and D^0 mass for the $D^* \rightarrow D^0[\rightarrow K^+ \pi^- \pi^0] \pi^+$ decays.

108 References

- 109 1. M. Gronau, Phys. Lett. B **627**, 82 (2005).
 110 2. F. Abudinén *et al.* (Belle II Collaboration), Eur. Phys. J. C **82**, 283 (2022).
 111 3. M. Gronau and D. London, Phys. Rev. Lett. **65**, 3381 (1990).
 112 4. M. Gronau and D. London, Phys. Lett. B, **253(3)**, 483–488(1991).
 113 5. M. Gronau and D. Wyler, Phys. Lett. B, **265(1)**, 172–176 (1991).
 114 6. Z. Ligeti Y. Grossman and A. Soffer, Phys. Rev. D, **67**, 071301 (2003).
 115 7. T. Keck, [arXiv:1609.06119](https://arxiv.org/abs/1609.06119).